

Comparative analysis of maca (*Lepidium meyenii*) proteome profiles reveals insights into response mechanisms of herbal plants to high-temperature stress

Wei Fan (✉ fanwei1128@aliyun.com)

Yunnan Agricultural University

Zhan Qi Wang

Huzhou University

Qi Ming Zhao

Yunnan Agricultural University

Xueting Zhong

Huzhou University

Li Xiao

Huzhou University

Li Xuan

Yunnan Agricultural University

Chou Fei Wu

Huzhou University

Li Qin Zhang

Huzhou University

Yang Tian

Yunnan Agricultural University

Research article

Keywords: High-temperature stress, Maca, Molecular mechanism, Stress response, Tandem mass tag

Posted Date: April 6th, 2020

DOI: <https://doi.org/10.21203/rs.3.rs-19357/v1>

License:  This work is licensed under a Creative Commons Attribution 4.0 International License. [Read Full License](#)

Version of Record: A version of this preprint was published at BMC Plant Biology on September 16th, 2020. See the published version at <https://doi.org/10.1186/s12870-020-02645-4>.

Abstract

Background High-temperature stress (HTS) is one of the main environmental stresses that limit plant growth and crop production in agricultural systems. Maca (*Lepidium meyenii*) is an important high-altitude herbaceous plant adapted to a wide range of environmental stimuli such as cold, strong wind and UV-B exposure. However, it is an extremely HTS-sensitive plant species. Thus far, there is limited information about gene/protein regulation and signaling pathways related to the heat stress response in maca. In this study, proteome profiles of maca seedlings exposed to HTS for 12 h were investigated using a tandem mass tag (TMT)-based proteomic approach.

Results In total, 6,966 proteins were identified, of which 379 showed significant alterations in expression following HTS. Bioinformatics analyses indicated that protein processing in endoplasmic reticulum was the most significantly up-regulated metabolic pathway following HTS. Quantitative RT-PCR (qRT-PCR) analysis showed that the expression levels of 21 genes encoding proteins mapped to this pathway were significantly up-regulated under HTS. These results show that protein processing in the endoplasmic reticulum may play a crucial role in the responses of maca to HTS.

Conclusions Our proteomic data can be a good resource for functional proteomics of maca and our results may provide useful insights into the molecular response mechanisms underlying herbal plants to HTS.

Background

Maca (*Lepidium meyenii* Walp) is an herbal plant of the Brassicaceae family, natively cultivated in the central highlands of the Peruvian Andes [1]. Due to its potential health benefits and valuable medicinal properties, maca has generated great interest in pharmacological and nutritional research and been introduced to many places around the world, which make it an attractive plant for the nutraceutical industry in recent years [2]. Because it is cultivated at altitudes of up to 3500 to 4500 m, maca possesses robust tolerance to extreme environmental stresses such as cold, strong wind and UV-B exposure [1]. Nevertheless, it is extremely sensitive to heat stress [1]. Thus far, there is limited information about gene/protein regulation and signaling pathways related to the heat stress response (HSR) in maca.

Under climate change, high temperatures are believed to be a serious threat to crop yields due to their negative effects on plant growth and development [3]. In recent years, extreme temperatures have occurred more frequently and with more intensity due to global warming. High-temperature stress (HTS), which is also known as heat stress, is a complex function of temperature intensity, duration and rate of increase [4]. Under HTS, high temperatures frequently cause not only direct damage that includes protein denaturation, aggregation and increase in membrane lipid fluidity, but also indirect damage that includes inactivation of enzymes in chloroplasts and mitochondria, disruption of protein homeostasis, and loss of membrane integrity [5]. These damages further result in a decline in photosynthetic rate, disruption of water balance and protein homeostasis, decrease in ion flux, production of reactive oxygen species (ROS), and destruction of hormone levels and cell structure [6]. These effects eventually result in growth inhibition and developmental retardation in plants.

It has been shown that heat stress response (HSR)-mediated tolerance mechanisms are key strategies to counter the effects of HTS on plants [5]. HSRs can raise numerous proteins that are produced from a specific set of HTS-responsive genes [7]. Therefore, the identification of genes and/or proteins involved in HSRs is crucial to understand the molecular mechanisms of plant response strategies to HTS. To date, although several studies have investigated plant responses to HTS in tomato, grape, rice, and wheat using transcriptomic or proteomic approaches [6,8], the molecular-level mechanisms underlying plant responses to HTS are still not fully understood, at least in herbal plants.

Tandem mass tag (TMT)-based proteomic analysis is a robust approach that extensively explores protein expression profiles and provides integrated information about individual proteins [9]. This advanced technology can be employed to determine the relative abundance of proteins between the control and treatment groups [10]. Over the past decade, the TMT-based proteomic approach has been broadly employed to explore differentially expressed proteins (DEPs) in plant

development and stress responses [-]. However, this approach has not yet been applied to investigate the molecular mechanisms of the responses of herbal plants to HTS.

In this study, a TMT-based comparative proteome analysis of maca was carried out to explore the molecular mechanisms responsible for high-temperature responses. Based on these measurements and bioinformatics analysis, we found that the 'protein processing in endoplasmic reticulum' pathway was the most significantly up-regulated metabolic process following HTS. The transcription of genes encoding 21 proteins involved in this pathway was further examined by qRT-PCR and each mRNA was found to be markedly up-regulated in maca seedlings exposed to HTS. These findings advance our understanding of crucial aspects of the molecular mechanisms underlying the responses to HTS in higher plants.

Results And Discussion

Effects of HTS on morphology and physiology of maca seedlings

Previous reports have shown that HTS frequently disturbs cellular homeostasis and can result in drastic reductions in the growth, development of plants, which can lead to death [1]. In this study, to examine the effects of HTS on the morphology and physiology of maca, two-week-old seedlings were treated at 42 °C for 0–24 h. As shown in Fig. 1a, the leaves of the seedlings exhibited chlorosis and wilted with prolongation of HTS treatment. This finding is consistent with previous phenotypes observed in other plant species subjected to HTS [13,14], indicating that HSRs were successfully induced. To validate the morphological phenotypes displayed in Fig. 1a, we also measured chlorophyll, malondialdehyde and soluble sugar contents, as well as total antioxidant capacity in maca seedlings under HTS. A significant decrease in chlorophyll content in the maca seedling leaves was detected under HTS after 24 h (Fig. 1b). Malondialdehyde is a product of membrane lipid peroxidation and increasing malondialdehyde content in cells indicates damage of plant cell membranes [15]. Compared with that in the control seedlings, malondialdehyde content was markedly increased and almost doubled in the maca seedlings following HTS for 24 h (Fig. 1c). As expected, the soluble sugar content and total antioxidant capacity in the leaves of maca seedlings were dramatically increased as HTS treatment time progressed (Fig. 1d and e). These findings corroborate previous studies showing that plants grown under HTS have increased sugar content and antioxidant capacity, which may be used by the plants to cope with HTS [16].

Proteomic expression profiles in maca seedlings under HTS

To determine the early-stage proteomic alterations of maca in response to HTS, we employed a TMT-based proteomic approach (Fig. 2a) and explored the comprehensive protein profiles of maca seedlings grown under control (25 °C) or HTS (42 °C) conditions for 12 h. As a result, 60,163 peptide spectra matched to the database and produced 55,426 peptides (Additional file 1), which were assembled into 6,966 non-redundant protein species (Additional file 2) at a 1% protein level FDR [17]. Compared with the control plants, 356 proteins from biological replicate 1 (Replicate 1), 352 proteins from biological replicate 2 (Replicate 2), and 350 proteins from biological replicate 3 (Replicate 3) displayed differential alterations in abundance following HTS, with a subset of 300 proteins detected in all three replicates (Fig. 2b). Furthermore, a scatter plot analysis of the ratios for each DEP was performed to assess reproducibility of the three biological replicates. Notably, the regression slope of the linear regression analyses between different replicates reached 0.97 (Fig. 2c–e), suggesting that the TMT proteomic data from different replicates are quite reproducible. Thus, in our study, the DEPs detected in two of three biological replicates were identified as significant DEPs (SDEPs). As a result, 379 SDEPs (Additional file 3) were identified in the leaves of maca seedlings following HTS, which included 215 up-regulated and 164 down-regulated proteins (Fig. 2f). Taken together, these results suggest that HTS causes a comprehensive change in proteome profiling of maca and, in turn, maca seedlings dramatically alter the levels of proteins putatively responding to HTS.

Furthermore, a gene ontology (GO) analysis of the SDEPs was also performed as described previously [16]. As shown in Fig. 3a, the SDEPs were divided according to their GO terms into molecular function, cellular component and biological

process. For molecular function, 36.1%, 35.9%, and 2.4% of the identified SDEPs were grouped under the terms 'binding', 'catalytic activity', and 'transporter activity', respectively (Fig. 3a). For biological process, 35.6%, 23.0%, and 18.7% of the identified SDEPs were the terms 'metabolic process', 'cellular process', and 'single-organism process', respectively (Fig. 3a). For cellular component, 'cell', 'membrane', and 'organelle' were the three most abundant terms, which accounted for 6.6%, 4.5%, and 2.9% of the SDEPs, respectively (Fig. 3a). The SDEPs were also grouped according to their subcellular localizations. As shown in Fig. 3b, more than 9 subcellular components were identified and the SDEPs were mainly located in the chloroplast (34.9%), cytosol (28.0%), and nucleus (20.6%). A small number of SDEPs were located, for example, in the plasma membrane, extracellular, mitochondria, endoplasmic reticulum, cytoskeleton, and vacuolar membrane (Fig. 3b). Moreover, using the eukaryotic orthologous group (KOG) classification, the SDEPs could be divided into 21 KOG functional categories. The three most highly represented categories were 'posttranslational modification, protein turnover, chaperones', 'carbohydrate transport and metabolism', 'secondary metabolites biosynthesis, transport and catabolism' but, except for the category of 'general function prediction only'. Interestingly, 99 SDEPs (26.1%) were classified into 'posttranslational modification, protein turnover, chaperones', which contained the most of the HTS-responsive proteins (Fig. 3c).

Since a goal of our proteomic analysis was to investigate the proteins in maca implicated in response to HTS and the associated response mechanisms, we classified the SDEPs according to the functional categories as described previously [1]. As shown in Fig. 2g, the SDEPs had a broad range of important biological functions in stress response, defense response, transcription, metabolism, protein homeostasis, cell growth/division, photosynthesis, secondary metabolism, cell structure, signal transduction, transporter, intracellular traffic and unknown functions. The SDEPs were found to be chiefly involved in stress response (33.5%), defense response (8.2%), transcription (7.4%) and metabolism (7.1%). These results are consistent with previous proteomic studies showing that HTS can up-regulate proteins involved in stress and defense, metabolism, protein homeostasis and cell growth/division in *Oryza sativa* [2], *Lycopersicon esculentum* [13] and *Pyropia haitanensis* [1]. Although the proteins identified in our study represent only a tiny proportion of the maca proteome, the identification of these HTS-responsive proteins may afford new insights into the response mechanisms of herbal plants to HTS. Some of the HTS-responsive proteins identified in the present study, which are implicated in the critical biological processes, are further discussed below.

Stress and defense responses. Plants have evolved various survival stress and defense responses to deal with environmental stresses [27]. Plants frequently require a battery of proteins participating in HSRs to adapt to the high-temperature conditions [1]. Previous studies have reported that heat shock proteins (HSPs) are major functional proteins induced by HTS [5,31]. In the present study, we found 127 SDEPs implicated in the stress response of maca seedlings to HTS, 42 of which were HSP-related proteins (Additional file 3). Interestingly, in our TMT proteomic data, all of these 42 HSP-related proteins were found to be significantly up-regulated under HTS (Additional file 3). These findings are consistent with previous proteomic studies showing that a number of HSPs involved in HSRs are dramatically up-regulated following HTS [6,29]. This indicates that maca seedlings initiate an extensive set of HSP-mediated HSRs during HTS and this may help plants to survive in high temperatures.

Beside the proteins associated with HSRs, 31 SDEPs related to defense responses were also identified in response to HTS, and 13 of them were found to be dramatically increased following HTS. For example, the expression of a thionin (Lmscaffold352.114), two BCL-2-associated athanogenes (Lmscaffold251.178 and Lmscaffold358.358), a DMR6 (Lmscaffold467.737), and a Mal d 1-associated protein (Lmscaffold18.354) was > 2-fold higher in HTS-treated maca seedlings than in the control plants (Additional file 3). These suggest that mild HTS may have positive roles in the resistance of plants to biotic stresses such as pathogen attacks. These findings are in agreement with previous reports showing that elevated temperatures can enhance the RNAi-mediated viral immunity, quantitative resistance traits, and PAMP-triggered immunity and increase the resistance of plants to Geminiviridae [1], *Puccinia striiformis* [1], bacteria [1] and RNA viruses [1].

Transcription. Recent studies have demonstrated that a complex transcriptional regulatory network mediated by various transcriptional regulators is implicated in plant responses to HTS [5]. Among these, transcription factors (TFs) have well established roles in HTS signaling and participate in regulating the expression of genes involved in HSRs []. In our study, 28 SDEPs associated with transcription were identified, and 19 of them were up-regulated in maca seedlings following HTS (Additional file 3). Among these up-regulated proteins, 7 of which were TFs that included a MBF1C (Lmscaffold306.354), AF1 (Lmscaffold603.40), HSFA2 (Lmscaffold26.42), WRKY transcription factor 70 (Lmscaffold455.415), transcription factor DIVARICATA (Lmscaffold353.74), transcription factor HY5 (Lmscaffold9.304) and alpha NAC TF (Lmscaffold299.549) (Additional file 3). In Arabidopsis, MBF1C was demonstrated to accumulate rapidly in leaves and act as a TF to control the expression of 36 downstream genes during HTS []. In grape plants, both the mRNA and protein levels of MBF1C are reported to be significantly induced by HTS and play a crucial role in regulating the heat shock transcription factor-HSP pathway in the thermotolerance of grapes [6,]. In our TMT proteomic data, the MBF1C was up-regulated by approximately 3.9-fold in maca seedlings following HTS. This suggests that MBF1C is also a key regulator in controlling the HSRs of maca to HTS. Furthermore, a HSFA2 was also identified to be increased by approximately 2.6-fold in maca seedlings following HTS (Additional file 3). This finding aligns with previous studies reporting that HSFA2 is an important transcriptional regulator and is essential for HSRs in Arabidopsis [] and tomato []. More interestingly, we also detected that the abundance of a transcription factor HY5 increased by approximately 1.8-fold upon HTS (Additional file 3). To the best of our knowledge, this is the first time that HY5 has been identified to be implicated in HTS responses using a proteomic approach. HY5 is frequently believed to be involved in plant growth and development, protein degradation, and photomorphogenesis induced by both visible light and UV-B radiation, as well as in the biosynthesis of flavonoids induced by biotic and abiotic stresses []. We surmised that the up-regulation of maca HY5 may function to activate the flavonoid biosynthesis pathway to respond to HTS, because a recent report showed that it can reduce HTS-induced ROS accumulation and inhibition of pollen tube growth in tomato []. However, Delker et al. [] reported that HY5 negatively controls the thermomorphogenesis of Arabidopsis to elevated temperatures via degradation of the basic-helix-loop-helix transcription factor phytochrome interacting factor 4, although there are cases where this effect is not evident. Thus, the exact role of HY5 in the HSRs of maca requires further examination in the future.

Metabolism and secondary metabolism. Previous reports have demonstrated that the down-regulation of metabolism is a generalized adaption response to HTS in plants [7,29]. In the present study, 27 metabolism-related SDEPs were identified and 25 of them were decreased in maca seedlings following HTS (Additional file 3). This is in line with previous transcriptomic data which showed that a specific cluster of genes, which are involved in the metabolism of carbohydrates, amino acids and lipids, are significantly decreased to adapt to the reduced need of primary metabolic products under HTS [6,11,14]. Furthermore, 13 SDEPs involved in secondary metabolism were identified in the present study. Similar to the expression patterns of metabolism-related proteins, most of these secondary metabolism-associated proteins were down-regulated in maca seedlings in response to HTS (Additional file 3). These observations suggest that maca seedlings can alter their metabolic pathways via down-regulating the expression of proteins to allow them to survive HTS.

Protein homeostasis. Previous studies have shown that protein homeostasis also plays important roles in regulating the HSRs of plants to HTS [7]. In the present study, we identified 25 SDEPs related to protein homeostasis, which are involved in both protein biosynthesis and proteolysis (Additional file 3). Among these, 16 SDEPs (Lmscaffold34.282, Lmscaffold78.160, Lmscaffold36.276, Lmscaffold629.27, Lmscaffold45.1237, Lmscaffold195.283, Lmscaffold108.65, Lmscaffold1844.436, Lmscaffold152.33, Lmscaffold519.48, Lmscaffold234.199, Lmscaffold45.305, Lmscaffold629.45, Lmscaffold291.247, Lmscaffold356.274, and Lmscaffold468.226) implicated in protein ubiquitination or degradation and two SDEPs (Lmscaffold37.599 and Lmscaffold127.69) involved in the regulation of protein translation increased their protein abundance in maca seedlings under HTS (Additional file 3). Interestingly, the accumulation levels of an ATP-dependent zinc metalloprotease FTSH 6 (FTSH6) (Lmscaffold629.27) and six ClpB/HSP101s (Lmscaffold34.282, Lmscaffold78.160, Lmscaffold195.283, Lmscaffold108.65, Lmscaffold1844.436, and Lmscaffold629.45) whose functions are related to proteolysis were increased more than 1.7-fold in maca seedlings following HTS, indicating that protein degradation is tightly controlled during HTS. Consistently, a recent study has demonstrated that Arabidopsis FTSH6 is

induced by HTS and accumulates in the plastid where it joins with HSP21 to form a plastidial FTSH6-HSP21 control module to regulate thermomemory in plants []. Actually, several studies have reported that ClpB/HSP101s, which have an ATP-dependent Clp protease activity, are induced by HTS and have been implicated in the acquisition of thermotolerance in plants []. Furthermore, we also found a BnaC02g00130D protein (Lmscaffold257.194), ATP-dependent Clp protease ATP-binding subunit CLPT2 (Lmscaffold215.106), eukaryotic translation initiation factor 2A (Lmscaffold34.174), nicastrin (Lmscaffold284.100), eukaryotic aspartyl protease family protein (Lmscaffold123.13), peptidase M1 family protein (Lmscaffold971.184), and a rolyl oligopeptidase family protein (Lmscaffold498.394) involved in protein translation and proteolysis were down-regulated in maca seedlings in response to HTS (Additional file 3). Overall, these data indicate that maca is able to modulate protein homeostasis to improve survival during HTS.

Moreover, in this study, we also identified various other proteins that were associated with cell growth/division, photosynthesis, cell structure, signal transduction, transporters, and intracellular traffic (Additional file 3). They also may have important roles in the regulation of HSRs of maca seedlings to HTS. Overall, our proteomic data provided here improve the understanding of the molecular mechanisms by which maca tolerates HTS, although the precise functions of these putative proteins remain to be fully examined.

Enrichment analysis of the SDEPs of maca seedlings in response to HTS

To gain more information about the potential functions of these HTS-responsive SDEPs, a GO enrichment analysis was conducted as described previously [16]. As shown in Fig. 4a, 27 GO terms covering 252 SDEPs were enriched. For the biological process category, 'inositol metabolic process', 'polyol biosynthetic process', and 'alcohol biosynthetic process' were the three most significantly enriched GO terms; For the molecular function category, the top three enriched GO terms were 'inositol-3-phosphate synthase activity', 'chaperone binding', and 'intramolecular lyase activity'. For the cellular component category, the most enriched GO terms were 'external encapsulating structure', 'cell wall', and 'organelle inner membrane'. Furthermore, protein domain enrichment analysis showed that 'hsp20-like chaperone', 'alpha crystallin/hsp20 domain', 'heat shock protein 70kD, peptide-binding domain', 'clp ATPase, C-terminal', and 'clp, N-terminal' were the top five significantly enriched domains (Fig. 4b).

Moreover, to further investigate the significantly changed metabolic pathways of maca plants under HTS, we also performed an enrichment analysis based on KEGG terms as described previously [27]. A Fisher's exact test showed that 13 KEGG pathways were significantly enriched following HTS (Table 1). It is interesting that 'protein processing in endoplasmic reticulum', 'metabolic pathways', 'biosynthesis of secondary metabolites' and 'porphyrin and chlorophyll metabolism' were dramatically changed in maca seedlings following HTS (Table 1). Additionally, the pathways 'sulfur metabolism', 'linoleic acid metabolism', 'inositol phosphate metabolism', 'thiamine metabolism', 'endocytosis', 'starch and sucrose metabolism', 'glutathione metabolism', and 'cysteine and methionine metabolism', also displayed P-values < 0.05 (Table 1).

Table 1
Representative HTS-responsive metabolic pathways enriched by KEGG pathway analysis.

Serial no.	KEGG pathway ^a	KEGG ID	Mapping	Background	All mapping	All background	Fold enrichment	Fisher's exact test P-values ^b
1	Protein processing in endoplasmic reticulum	ath04141	46	185	149	2859	4.77	1.26×10^{-12}
2	Biosynthesis of secondary metabolites	ath01110	30	798	56	2859	1.92	3.86×10^{-5}
3	Metabolic pathways	ath01100	42	1398	56	2859	1.53	5.26×10^{-5}
4	Porphyrin and chlorophyll metabolism	ath00860	10	46	149	2859	4.17	8.81×10^{-5}
5	Fatty acid elongation	ath00062	3	9	56	2859	17.02	5.50×10^{-4}
6	Sulfur metabolism	ath00920	2	40	8	2859	17.87	5.07×10^{-3}
7	Linoleic acid metabolism	ath00591	2	7	56	2859	14.59	7.43×10^{-3}
8	Inositol phosphate metabolism	ath00562	3	33	49	2859	5.3	1.80×10^{-2}
9	Thiamine metabolism	ath00730	2	17	36	2859	9.34	1.86×10^{-2}
10	Endocytosis	ath04144	4	83	36	2859	3.83	1.92×10^{-2}
11	Cysteine and methionine metabolism	ath00270	5	91	56	2859	2.81	3.11×10^{-2}
12	Starch and sucrose metabolism	ath00500	5	94	56	2859	2.72	3.52×10^{-2}
13	Phenylpropanoid biosynthesis	ath00940	4	67	49	2859	3.48	3.71×10^{-2}
^a All KEGG pathways were retrieved from KEGG release 88.2 on November 1, 2018.								
^b Pathways were considered as significantly enriched at $P < 0.05$ and the pathways with a P-value higher than 0.05 were not listed.								

For cluster analysis, the SDEPs were classified into four groups according to their quantification ratios (Fig. 5a) and then subjected to KEGG-based enrichment. As shown in Fig. 5b, the SDEPs in Q1 ($0 < \text{ratio} \leq 0.500$) were predominantly involved in 'porphyrin and chlorophyll metabolism' and 'sulfur metabolism'; the SDEPs in Q2 ($0.500 < \text{ratio} \leq 0.667$) were closely

related to 'metabolic pathways', 'biosynthesis of secondary metabolites', 'fatty acid elongation', 'porphyrin and chlorophyll metabolism', 'linoleic acid metabolism', 'starch and sucrose metabolism' and 'cysteine and methionine metabolism'; the SDEPs in Q3 ($1.500 < \text{ratio} \leq 2.000$) were exclusively related to 'protein processing in endoplasmic reticulum', 'thiamine metabolism', 'endocytosis' and 'glutathione metabolism'; and the SDEPs in Q4 ($\text{ratio} > 2.000$) were chiefly related to 'protein processing in endoplasmic reticulum' and 'inositol phosphate metabolism'. These results indicate that the SDEPs divided into Q3 and Q4, which were up-regulated following HTS, are principally involved in 'protein processing in endoplasmic reticulum', 'inositol phosphate metabolism' and 'thiamine metabolism', but especially in 'protein processing in endoplasmic reticulum'. This is consistent with previous reports that several 'protein processing in endoplasmic reticulum' related genes/proteins are induced by HTS in various plant species [29]. A summary view of the 'protein processing in endoplasmic reticulum' pathway is shown in Fig. 5c.

PPI networks for the SDEPs of maca seedlings in response to HTS

PPI networks were further constructed to predict the potential biological functions of the HTS-responsive proteins in maca seedlings. A total of 101 SDEPs (62 up-regulated and 39 down-regulated, Additional file 4), which had confidence scores ≥ 0.7 (high confidence), were assigned to the PPI networks. As shown in Fig. 6a, two important cascades of biochemical processes, specifically 'protein processing in endoplasmic reticulum' and 'porphyrin and chlorophyll metabolism', were identified. Interestingly, most of the SDEPs implicated in the 'protein processing in endoplasmic reticulum' pathway had an increase in their accumulation following HTS (Fig. 6a and Additional file 5). In contrast, the SDEPs implicated in the 'porphyrin and chlorophyll metabolism' pathway were decreased (Fig. 6a and Additional file 6). These findings corroborate the above-mentioned results, which show that the 'protein processing in endoplasmic reticulum' pathway was significantly enhanced following HTS (Fig. 5b), and that there was an obvious decrease in chlorophyll content in the leaves of maca seedlings under HTS (Fig. 1b).

qRT-PCR validation

Since the earlier TMT proteomic data, enrichment and PPI analyses showed that the 'protein processing in endoplasmic reticulum' pathway might play an essential role in HTS tolerance in maca seedlings (Figs. 5b and 6a, and Additional file 3), we further examined this pathway by determining the expression pattern of 21 related genes. Total RNA was extracted from maca seedlings grown under control or HTS conditions for 12 h, and subjected to qRT-PCR analysis. As shown in Fig. 6b, all of 21 SDEPs were significantly induced by HTS at the mRNA level and 17 of them were up-regulated more than 3-fold. These qRT-PCR results are in agreement with the TMT proteomic data (Fig. 6c and Additional file 3). This obvious up-regulation of proteins (genes) implicated in the 'protein processing in endoplasmic reticulum' pathway indicates a significant enhancement of protein biosynthesis, degradation and folding, which could be used by the plants to cope with HTS. These results suggest that the up-regulation of proteins correlates with the increase in their transcript abundance.

Conclusions

Incubations at 42 °C for 12 h caused significant morphological and physiological changes in maca seedlings, and these were manifested as decreased chlorophyll content, increased malondialdehyde content, increased soluble sugar content, and increased total antioxidant capacity. Proteomic analysis showed that the levels of 379 proteins were differentially changed by HTS. Bioinformatics and qRT-PCR analyses indicated that protein processing in the endoplasmic reticulum is the most significantly enhanced KEGG pathway in maca in response to HTS. These experimental data afford some new insights which may provide a deeper understanding of the molecular responses of herbal plants to HTS. These results also reveal that the combination of proteomics, bioinformatics and qRT-PCR analysis is an effective method to investigate response mechanisms to HTS in higher plants.

Methods

Plant material, culture and HTS treatment

Maca (*Lepidium meyenii* Walp) cultivar 'Wumeng' (Breeding and preservation by Yunnan Agricultural University, YunR-SV-LM-045-2017) was used in this study. For cultivation, the seeds were surface-sterilized with 1% (v/v) NaClO for 10 min, followed by five rinses in sterile water, and immersed in distilled water overnight. After germination, the seeds were transferred to 60-well plates in 8-L plastic containers with one-fifth-strength Hoagland solution (pH 5.5), which was replenished every other day. The seedlings were grown in a green house at 25 °C under a 16/8 h (light/dark) photoperiod with a light intensity of 150–180 $\mu\text{E m}^{-2} \text{s}^{-1}$. For the HTS treatment, the seedlings were grown in a growth chamber at 42 °C for 0–24 h under continuous illumination at a light intensity of 150–180 $\mu\text{E m}^{-2} \text{s}^{-1}$ as described previously [21,22]. Seedlings grown at 25 °C under similar illumination were used as the controls. The treatments were repeated three times.

Determination of chlorophyll and soluble sugar contents

Chlorophyll was extracted from 0.2 g of fresh leaves by grinding them in 2.5 mL of ice-cold 80% acetone and determined as described by Zhou et al. [1]. The chlorophyll content was recorded as chlorophyll content per gram fresh weight (FW). Soluble sugar content was measured as described by Wang et al. [2]. The sugar concentration was determined at A_{625} and recorded as soluble sugar per gram FW. The experiments were repeated three times.

Malondialdehyde concentration and total antioxidant capacity measurement

Malondialdehyde concentration was measured using the following formula: malondialdehyde ($\mu\text{mol g}^{-1} \text{FW}$) = $[6.45 \times (A_{532} - A_{600}) - 0.56 \times A_{450}] \times V/W$, in which A_{532} , A_{600} and A_{450} are the absorbances at 532, 600 and 450 nm, respectively; and V is the volume of extraction; and W is the FW of the sample [3]. Total antioxidant capacity was determined using the ferric reducing antioxidant power (FRAP) assay as described previously [4]. The total antioxidant capacity was reported as $\mu\text{mol Fe}^{2+}$ per gram FW. The experiments were repeated three times.

Protein extraction and proteomic analysis

In this study, three independent biological replicates were conducted for each treatment. Protein from leaf samples was extracted as described by Wang et al. [27]. The protein samples were digested labeled using the TMT Isobaric Mass Tagging Kit (Thermo Fisher Scientific, USA). In detail, the peptides from the control samples were labeled with TMT reagents 126, 127, and 128, and those from the HTS-treated samples were labeled with TMT reagents 129, 130, and 131. High-performance liquid chromatography (HPLC) fractionation was conducted as described by Zhan et al. [16] and liquid chromatography-tandem mass spectrometry (LC-MS/MS) was carried out with an automated Easy-nLC 1000 UPLC system coupled to a Q-Exactive™ Plus mass spectrometer (Thermo Fisher Scientific, USA) as described by Wang et al. [27]. All data were reported based on 99% confidence for peptide and protein identification as determined by a FDR of less than 1% as described previously [25,26]. The quantification ratio was calculated to assess the fold changes in the abundance of the proteins identified in HTS-treated (HTS) vs control (Cont) plants. Student's t-test adjusted by the Benjamini-Hochberg (BH) method [5] was used to identify significant ($P_{\text{adj}} < 0.05$) differences in the means of HTS and Cont seedlings among the three biological replicates. To be identified as being differentially expressed, a protein must have a fold-change ratio > 1.500 or < 0.667 , be detected in at least two of the three biological replicates, and pass the t-test with BH-adjusted $P_{\text{adj}} < 0.05$. Reproducibility analysis of the biological replicates was performed using analysis of variance of the differentially expressed protein (DEP) data as described previously [27].

Protein annotation, classification and enrichment analyses

GO and domain annotations were conducted as described by Zhan et al. [16]. The functional classification and enrichment analysis of SDEPs were carried out as described previously [27,49].

Protein-protein interaction (PPI) analysis

All the SDEPs were searched against the STRING database (v. 11.0, [http://string-db.org/cgi/about.pl? footer_active_subpage = references](http://string-db.org/cgi/about.pl?footer_active_subpage=references)) for PPI predictions. Interactions between proteins belonging to the data set were selected. Only the interactions having confidence scores ≥ 0.7 (high confidence) were fetched. The interaction network from STRING was visualized in Cytoscape (v. 3.6.1) [1].

qRT-PCR analysis

RNA extraction and qRT-PCR were carried out as described by Wang et al. [1]. Relative mRNA expression levels were calculated using the comparative C_T method [2]. Maca actin 2 (LmACT2) was used as an internal control [3]. The primers used for qRT-PCR analysis are listed in Additional file 7. The results were averages of three biological replicates.

Statistical analysis

The data represent means \pm standard deviation (SD) of three independent biological replicates. Student's t-test was performed in Microsoft Excel (v.2016, Microsoft Corp., USA) and a BH-adjusted [52] P-value less than 0.05 ($P_{adj} < 0.05$) was considered statistically significant as described previously [27].

Abbreviations

BH: Benjamini-Hochberg method; DEP: differentially expressed protein; FDR: false discovery rate; FRAP: ferric reducing antioxidant power; FW: fresh weight; GO: Gene Ontology; HPLC: high-performance liquid chromatography; HSP: heat shock proteins; HSR: heat stress response; HTS: high-temperature stress; KEGG: Kyoto Encyclopedia of Genes and Genomes; KOG: eukaryotic orthologous group; LC-MS/MS: liquid chromatography-tandem mass spectrometry; PPI: protein-protein interaction; qRT-PCR: quantitative RT-PCR; ROS: reactive oxygen species; SD: standard deviation; SDEP: significant differentially expressed protein; TF: transcription factor; TMT: tandem mass tag; XTH: xyloglucan endotransglucosylase/hydrolase.

Declarations

Ethics approval and consent to participate

Not applicable. The authors declared that experimental research works on the plants described in this paper comply with institutional, national and international guidelines.

Consent for publication

Not applicable.

Availability of data and materials

The datasets supporting the conclusions of this article are included within the article and its additional files. The mass spectrometry proteomics data reported in this paper have been deposited in the PRoteomics IDentifications (PRIDE) database (<http://www.ebi.ac.uk/pride/>) (accession number: PXD017843).

Competing interests

The authors declare that they have no competing interests.

Funding

This research was supported by the Major Science and Technique Programs in Yunnan Province (2017ZF004) and the Talent Foundation of Huzhou University, China (RK23069 and RK23070). There is no role of the funding body in the design of the study and collection, analysis, and interpretation of data and in writing the manuscript.

Authors' contributions

ZQW, YT and WF designed and supervised the project; QMZ, XZ, LX, LXM, and CFW performed the experiments; ZQW, LQZ and YT analyzed the data; ZQW, YT and WF wrote the manuscript. All authors read and approved the manuscript.

Acknowledgements

We are also grateful to PTM Bio company (Hangzhou, China) for technical support and Editage company (Shanghai, China) for English language editing.

Author details

¹ Key Laboratory of Vector Biology and Pathogen Control of Zhejiang Province, College of Life Sciences, Huzhou University, Huzhou 313000, China (ZQW, ZXT, XL, WCF and LQZ). ² State Key Laboratory of Conservation and Utilization of Bio-resources in Yunnan, The Key Laboratory of Medicinal Plant Biology of Yunnan Province, National & Local Joint Engineering Research Center on Germplasm Innovation & Utilization of Chinese Medicinal Materials in Southwest China, Yunnan Agricultural University, Kunming 650201, China (QMZ, WF). ³ College of Food Science and Technology, Yunnan Agricultural University, Kunming 650201, China (LXM, YT). ⁴ Huzhou central hospital, Huzhou University, Huzhou 313000, China (LQZ).

References

- [1.] Zhang J, Tian Y, Yan L, Zhang G, Wang X, Zeng Y, et al. Genome of plant maca (*Lepidium meyenii*) illuminates genomic basis for high-altitude adaptation in the central Andes. *Mol Plant*. 2016;9(7):1066–1077.
- [2.] Esparza E, Hadzich A, Kofer W, Mithöfer A, Cosio EG. Bioactive maca (*Lepidium meyenii*) alkamides are a result of traditional Andean postharvest drying practices. *Phytochemistry*. 2015;116:138–148.
- [3.] Huarancca Reyes T, Scartazza A, Pompeiano A, Guglielminetti L. Physiological responses of *Lepidium meyenii* plants to ultraviolet-B radiation challenge. *BMC Plant Biol*. 2019;19:186.
- [4.] Chen J, Zhang J, Lin M, Dong W, Guo X, Dong Y, et al. MGH: a genome hub for the medicinal plant maca (*Lepidium meyenii*). *Database*. 2018;2018: bay113.
- [5.] Ohama N, Sato H, Shinozaki K, Yamaguchi-Shinozaki K. Transcriptional regulatory network of plant heat stress response. *Trends Plant Sci*. 2017;22(1):53–65.
- [6.] Jiang J, Liu X, Liu C, Liu G, Li S, Wang L. Integrating omics and alternative splicing reveals insights into grape response to high temperature. *Plant Physiol*. 2017;173(2):1502–1518.
- [7.] Liu GT, Ma L, Duan W, Wang BC, Li JH, Xu HG, et al. Differential proteomic analysis of grapevine leaves by iTRAQ reveals responses to heat stress and subsequent recovery. *BMC Plant Biol*. 2014;14:110.
- [8.] Shao L, Shu Z, Sun SL, Peng CL, Wang XJ, Lin ZF. Antioxidation of anthocyanins in photosynthesis under high temperature stress. *J Integr Plant Biol*. 2007; 49(9):1341–1351.
- [9.] Ohama N, Kusakabe K, Mizoi J, Zhao H, Kidokoro S, Koizumi S, et al. The transcriptional cascade in the heat stress response of *Arabidopsis* is strictly regulated at the level of transcription factor expression. *Plant Cell*. 2016;28:181–201.
- [10.] Frank G, Pressman E, Ophir R, Althan L, Shaked R, Freedman M, et al. Transcriptional profiling of maturing tomato (*Solanum lycopersicum* L.) microspores reveals the involvement of heat shock proteins, ROS scavengers, hormones, and sugars in the heat stress response. *J Exp Bot*. 2009;60(13):3891–3908.

- [11.] Su P, Jiang C, Qin H, Hu R, Feng J, Chang J, et al. Identification of potential genes responsible for thermotolerance in wheat under high temperature stress. *Genes*. 2019;10(2):174.
- [12.] Thompson A, Schäfer J, Kuhn K, Kienle S, Schwarz J, Schmidt G, et al. Tandem mass tags: a novel quantification strategy for comparative analysis of complex protein mixtures by MS/MS. *Anal Chem*. 2003;75(18):1895–1904.
- [13.] Zhan X, Liao X, Luo X, Zhu Y, Feng S, Yu C, et al. Comparative metabolomic and proteomic analyses reveal the regulation mechanism underlying MeJA-induced bioactive compound accumulation in cutleaf groundcherry (*Physalis angulata* L.) hairy roots. *J Agric Food Chem*. 2018;66(25):6336–6347.
- [14.] Dhakarey R, Raorane ML, Treumann A, Peethambaran PK, Schendel RR, Sahi VP, et al. Physiological and proteomic analysis of the rice mutant *cpm2* suggests a negative regulatory role of jasmonic acid in drought tolerance. *Front Plant Sci*. 2017; 8:1903.
- [15.] Zhan Y, Wu Q, Chen Y, Tang M, Sun C, Sun J, et al. Comparative proteomic analysis of okra (*Abelmoschus esculentus* L.) seedlings under salt stress. *BMC Genomics*. 2019;20:381.
- [16.] Hasanuzzaman M, Nahar K, Alam MM, Roychowdhury R, Fujita M. Physiological, biochemical, and molecular mechanisms of heat stress tolerance in plants. *Int J Mol Sci*. 2013;14(5):9643–9684.
- [17.] Ding H, He J, Wu Y, Wu X, Ge C, Wang Y, et al. The tomato mitogen-activated protein kinase SIMPK1 is a negative regulator of the high-temperature stress response. *Plant Physiol*. 2018;177(2):633–651.
- [18.] Djanaguiraman M, Perumal R, Ciampitti IA, Gupta SK, Prasad PVV. Quantifying pearl millet response to high temperature stress: thresholds, sensitive stages, genetic variability and relative sensitivity of pollen and pistil. *Plant Cell Environ*. 2018;41(5):993–1007.
- [19.] Cheng L, Zou Y, Ding S, Zhang J, Yu X, Cao J, et al. Polyamine accumulation in transgenic tomato enhances the tolerance to high temperature stress. *J Integr Plant Biol*. 2009;51(5):489–499.
- [20.] Min L, Li Y, Hu Q, Zhu L, Gao W, Wu Y, et al. Sugar and auxin signaling pathways respond to high-temperature stress during anther development as revealed by transcript profiling analysis in cotton. *Plant Physiol*. 2014;164(3):1293–1308.
- [21.] Roitinger E, Hofer M, Köcher T, Pichler P, Novatchkova M, Yang J, et al. Quantitative phosphoproteomics of the ataxia telangiectasia-mutated (ATM) and ataxia telangiectasia-mutated and rad3-related (ATR) dependent DNA damage response in *Arabidopsis thaliana*. *Mol Cell Proteomics*. 2015;14(3):556–571.
- [22.] Zhong X, Wang ZQ, Xiao R, Wang Y, Xie Y, Zhou X. iTRAQ analysis of the tobacco leaf proteome reveals that RNA-directed DNA methylation (RdDM) has important roles in defense against geminivirus-betasatellite infection. *J Proteomics*. 2017;152:88–101.
- [23.] Wang ZQ, Zhou X, Dong L, Guo J, Chen Y, Zhang Y, et al. iTRAQ-based analysis of the *Arabidopsis* proteome reveals insights into the potential mechanisms of anthocyanin accumulation regulation in response to phosphate deficiency. *J Proteomics*. 2018;184:39–53.
- [24.] Gammulla CG, Pascovici D, Atwell BJ, Haynes PA. Differential proteomic response of rice (*Oryza sativa*) leaves exposed to high- and low-temperature stress. *Proteomics*. 2011;11(14):2839–2850.
- [25.] Shi J, Chen Y, Xu Y, Ji D, Chen C, Xie C. Differential proteomic analysis by iTRAQ reveals the mechanism of *Pyropia haitanensis* responding to high temperature stress. *Sci Rep*. 2017;7:44734.

- [26.] Saijo Y, Loo EP. Plant immunity in signal integration between biotic and abiotic stress responses. *New Phytol.* 2020;225:87–104.
- [27.] Kotak S, Larkindale J, Lee U, von Koskull-Döring P, Vierling E, Scharf KD. Complexity of the heat stress response in plants. *Curr Opin Plant Biol.* 2007;10(3):310–316.
- [28.] Chellappan P, Vanitharani R, Ogbe F, Fauquet CM. Effect of temperature on geminivirus-induced RNA silencing in plants. *Plant Physiol.* 2005;138(4):1828–1841.
- [29.] Fu D, Uauy C, Distelfeld A, Blechl A, Epstein L, Chen X, et al. A kinase-START gene confers temperature-dependent resistance to wheat stripe rust. *Science.* 2009;323(5919):1357–1360.
- [30.] Cheng C, Gao X, Feng B, Sheen J, Shan L, He P. Plant immune response to pathogens differs with changing temperatures. *Nat Commun.* 2013; 4:2530.
- [31.] Ma L, Huang X, Yu R, Jing XL, Xu J, Wu CA, et al. Elevated ambient temperature differentially affects virus resistance in two tobacco species. *Phytopathology.* 2016;106(1):94–100.
- [32.] Guo M, Liu JH, Ma X, Luo DX, Gong ZH, Lu MH. The plant heat stress transcription factors (HSFs): structure, regulation, and function in response to abiotic stresses. *Front Plant Sci.* 2016;7:114.
- [33.] Suzuki N, Sejima H, Tam R, Schlauch K, Mittler R. Identification of the MBF1 heat-response regulon of *Arabidopsis thaliana*. *Plant J.* 2011; 66(5):844–851.
- [34.] Carbonell-Bejerano P, Santa María E, Torres-Pérez R, Royo C, Lijavetzky D, Bravo G, et al. Thermotolerance responses in ripening berries of *Vitis vinifera* L. cv Muscat Hamburg. *Plant Cell Physiol.* 2013;54(7):1200–1216.
- [35.] Liu J, Sun N, Liu M, Liu J, Du B, Wang X, et al. An autoregulatory loop controlling *Arabidopsis* HsfA2 expression: role of heat shock-induced alternative splicing. *Plant Physiol.* 2013;162(1):512–521.
- [36.] Fragkostefanakis S, Mesihovic A, Simm S, Paupière MJ, Hu Y, Paul P, et al. HsfA2 controls the activity of developmentally and stress-regulated heat stress protection mechanisms in tomato male reproductive tissues. *Plant Physiol.* 2016;170(4):2461–2477.
- [37.] Gangappa SN, Botto JF. The multifaceted roles of HY5 in plant growth and development. *Mol Plant.* 2016;9(10):1353–1365.
- [38] Muhlemann JK, Younts TLB, Muday GK. Flavonols control pollen tube growth and integrity by regulating ROS homeostasis during high-temperature stress. *Proc Nat Acad Sci USA.* 2018;115(47):E11188–E11197.
- [39.] Delker C, Sonntag L, James GV, Janitza P, Ibañez C, Ziermann H, et al. The DET1-COP1-HY5 pathway constitutes a multipurpose signaling module regulating plant photomorphogenesis and thermomorphogenesis. *Cell Rep.* 2014;9(6):1983–1989.
- [40.] Sedaghatmehr M, Mueller-Roeber B, Balazadeh S. The plastid metalloprotease FtsH6 and small heat shock protein HSP21 jointly regulate thermomemory in *Arabidopsis*. *Nat Commun.* 2016;7:12439.
- [41.] Larkindale J, Vierling E. Core genome responses involved in acclimation to high temperature. *Plant Physiol.* 2008;146(2):748–761.
- [42.] Pulido P, Llamas E, Llorente B, Ventura S, Wright LP, Rodríguez-Concepción M. Specific Hsp100 chaperones determine the fate of the first enzyme of the plastidial isoprenoid pathway for either refolding or degradation by the stromal clp

protease in Arabidopsis. PLoS Genet. 2016;12(1):e1005824.

[43.] Sun P, Mao Y, Li G, Cao M, Kong F, Wang L, et al. Comparative transcriptome profiling of *Pyropia yezoensis* (Ueda) M.S. Hwang & H.G. Choi in response to temperature stresses. BMC Genomics. 2015;16:463.

[44.] Zhou Q, Yu Q, Wang Z, Pan Y, Lv W, Zhu L, et al. Knockdown of GDCH gene reveals reactive oxygen species-induced leaf senescence in rice. Plant Cell Environ. 2013;36(8):1476–1489.

[45.] Wang ZQ, Xu XY, Gong QQ, Xie C, Fan W, Yang JL, et al. Root proteome of rice studied by iTRAQ provides integrated insight into aluminum stress tolerance mechanisms in plants. J Proteomics. 2014;98:189–205.

[46.] Li G, Peng X, Xuan H, Wei L, Yang Y, Guo T, et al. Proteomic analysis of leaves and roots of common wheat (*Triticum aestivum* L.) under copper-stress conditions. J Proteome Res. 2013;12(11):4846–4861.

[47.] Xia Q, Wang L, Xu C, Mei J, Li Y. Effects of germination and high hydrostatic pressure processing on mineral elements, amino acids and antioxidants in vitro bioaccessibility, as well as starch digestibility in brown rice (*Oryza sativa* L.). Food Chem. 2017; 214:533–542.

[48.] Benjamini Y, Hochberg Y. Controlling the false discovery rate: a practical and powerful approach to multiple testing. J R Statist Soc B. 1995;57(1):289–300.

[49.] Shannon P, Markiel A, Ozier O, Baliga NS, Wang JT, Ramage D, et al. Cytoscape: a software environment for integrated models of biomolecular interaction networks. Genome Res. 2003;13(11):2498–2504.

[50.] Wang ZQ, Li GZ, Gong QQ, Li GX, Zheng SJ. OsTCTP, encoding a translationally controlled tumor protein, plays an important role in mercury tolerance in rice. BMC Plant Biol. 2015;15:123.

[51.] Schmittgen TD, Livak KJ. Analyzing real-time PCR data by the comparative CT method. Nat Protoc. 2008;3(6):1101–1108.

[52.] Shi Y, Su Z, Yang H, Wang W, Jin G, He G, et al. Alternative splicing coupled to nonsense-mediated mRNA decay contributes to the high-altitude adaptation of maca (*Lepidium meyenii*). Gene. 2019;694:7–18.

Figures

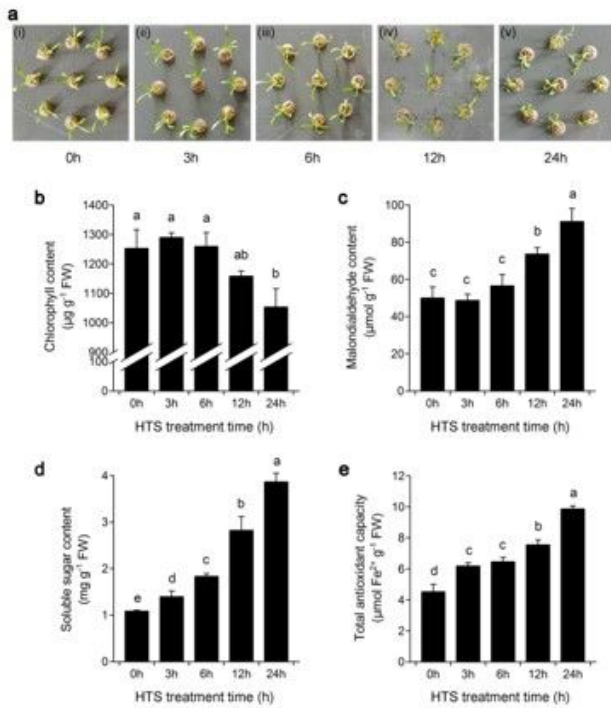


Figure 1

Effects of high-temperature stress (HTS) on morphology and physiology of maca seedlings. (a) Phenotype of maca seedlings under 42 °C for 0–24 h. (B–E) Impact of HTS on (b) chlorophyll content, (c) malondialdehyde content, (d) soluble sugar content and (e) total antioxidant capacity in the leaves of maca seedlings. The data are given as means \pm standard deviation (SD) of three biological replicates. Means with different letters are significantly different (Student's t-test, $P < 0.05$).

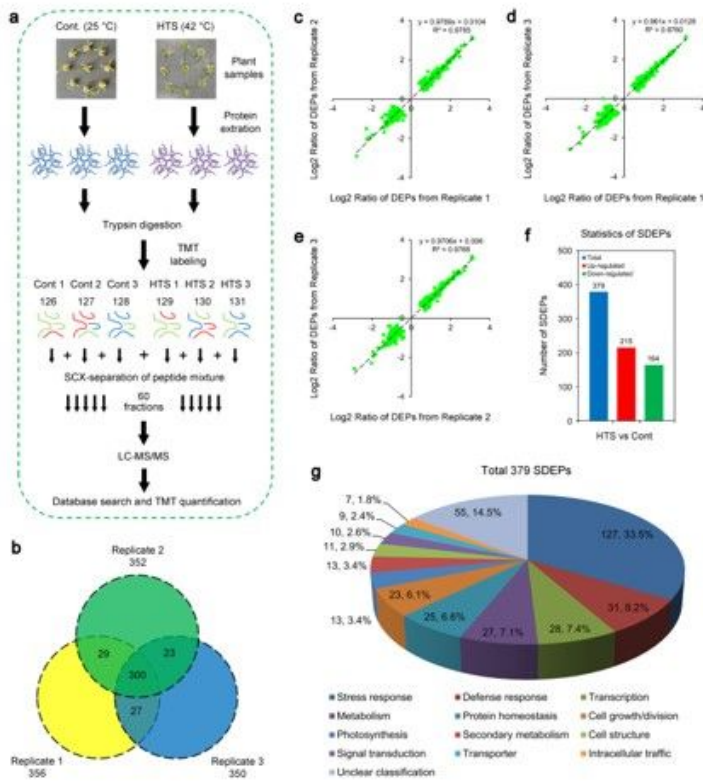


Figure 2

Proteomic analysis of maca seedlings in response to HTS. (a) Experimental scheme for the proteomic analysis. Two-week-old maca seedlings (cv. Wumeng) were treated with 42 °C or grown under control conditions for 12 h and proteins were extracted from three independent biological replicates per treatment. Extracted proteins were digested with trypsin and labeled with TMT reagents. Labeled peptides were fractionated by HPLC and fractions were further analyzed by reversed phase LC-MS/MS. (b) Venn diagram analysis of differentially expressed proteins (DEPs) identified in maca seedlings using three biological replicates. The numbers of the DEPs identified from different biological replicates are shown in the different segments. (c–e) Variance analyses of the DEPs from three biological replicates. (f) The numbers of total, up-regulated and down-regulated DEPs in leaves of maca seedlings under HTS. (g) Functional classification of the significant DEPs (SDEPs).

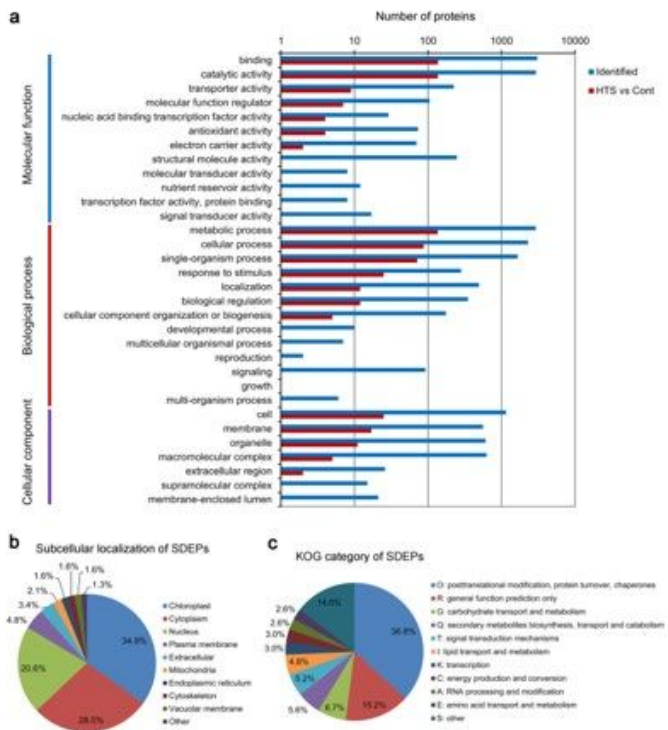


Figure 3

Classification information of the significant DEPs (SDEPs) of maca seedlings following HTS. (a) Gene ontology (GO) analysis of all identified proteins and SDEPs. All identified proteins and SDEPs were classified by GO terms based on their molecular function, biological process, and cellular component. (b) Subcellular localization analysis of the SDEPs. (c) Eukaryotic orthologous group (KOG) category classification of the SDEPs.

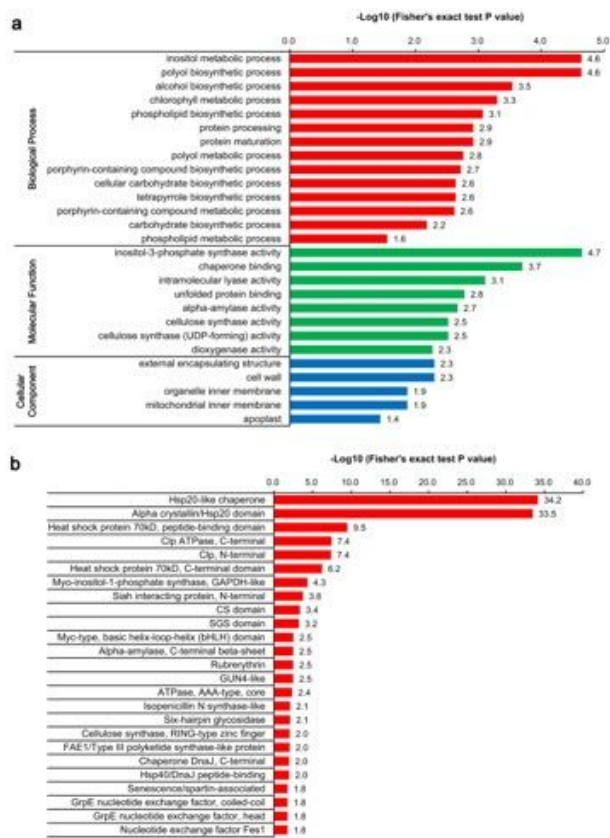


Figure 4

Gene ontology (GO) and protein domain enrichment analyses of the SDEPs in response to HTS. (a) GO enrichment analysis of the SDEPs. (b) Protein domain enrichment analysis of the SDEPs.

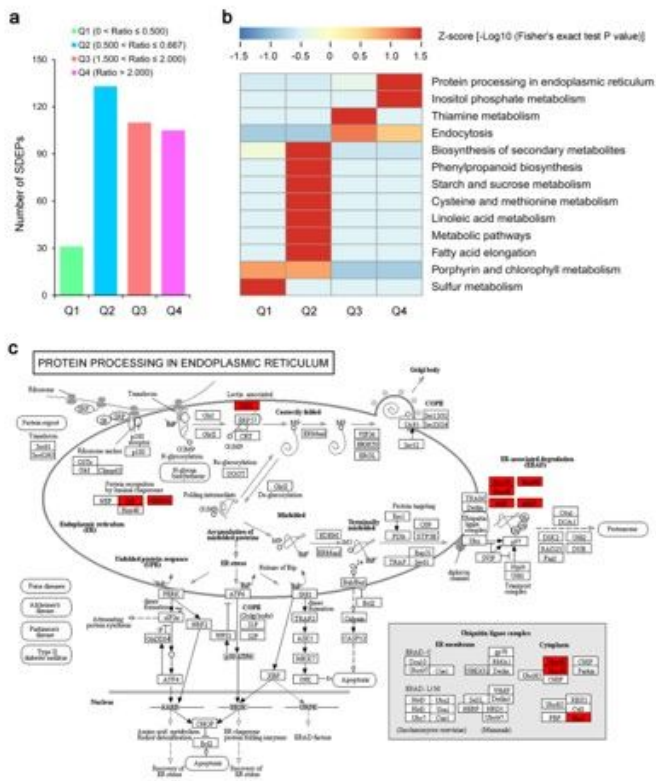


Figure 5

Kyoto Encyclopedia of Genes and Genomes (KEGG) enrichment analysis of the SDEPs responding to HTS. (a) Comparable group of the SDEPs based on their quantification ratios: Q1 ($0 < \text{ratio} \leq 0.500$), Q2 ($0.500 < \text{ratio} \leq 0.667$), Q3 ($1.500 < \text{ratio} \leq 2.000$) and Q4 ($\text{ratio} > 2.000$). (b) Significantly enriched KEGG pathways of the SDEPs. (c) Schematic representation of the SDEPs implicated in the 'protein processing in endoplasmic reticulum' pathway. Red boxes indicate the SDEPs identified under HTS.

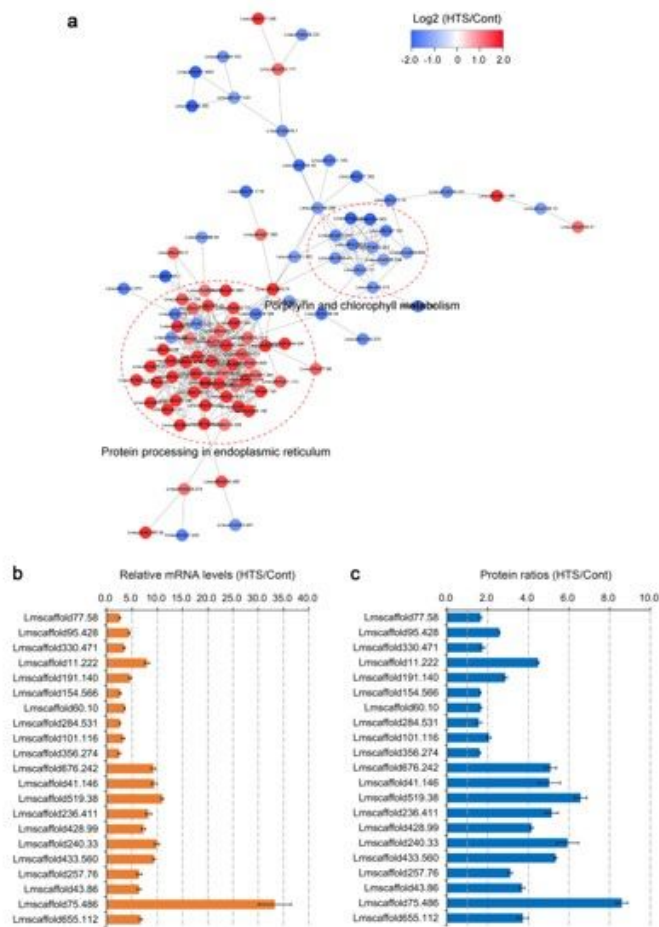


Figure 6

Protein-protein interaction (PPI) networks of the SDEPs and qRT-PCR analysis of gene expression levels. (a) PPI networks of the SDEPs were analyzed using STRING database (v. 11.0) and Cytoscape software (v. 3.6.1). The color bar indicates protein quantitation of Log₂ (HTS/Cont) ratio. Red balls indicate up-regulated SDEPs and blue balls indicate down-regulated SDEPs. Red cycles indicate the two enriched protein-protein interaction clusters. (b) qRT-PCR analysis of gene expression levels. Twenty-one SDEPs implicated in the 'protein processing in endoplasmic reticulum' pathway were selected and subjected to qRT-PCR analysis using the same samples as for TMT proteomic data. LmACT2 was used as an internal reference. (c) Protein ratios of 21 SDEPs implicated in the 'protein processing in endoplasmic reticulum' pathway. The data are given as means \pm SD of three biological replicates.

Supplementary Files

This is a list of supplementary files associated with this preprint. Click to download.

- [TableS2.xlsx](#)
- [TableS3.xlsx](#)
- [TableS5.xlsx](#)
- [TableS6.xlsx](#)
- [TableS4.xlsx](#)

- [TableS1.xlsx](#)
- [TableS7.xlsx](#)